

# CNC centralized control for digitizing freeform surfaces by means of a conoscopic holography sensor integrated in a machining centre

Pablo Zapico<sup>a</sup>, Héctor Patiño<sup>b</sup>, Gonzalo Valiño<sup>b,1</sup>, Pedro Fernández<sup>b</sup>, J. Carlos Rico<sup>b</sup>

<sup>a</sup> Cybernetic Research Module  
University of León  
Campus de Vegazana, 24071 León, Spain

<sup>b</sup> Department of Construction and Manufacturing Engineering  
University of Oviedo  
Campus de Gijón, 33203 Gijón, Spain

<sup>1</sup> Corresponding author: e-mail address: [gvr@uniovi.es](mailto:gvr@uniovi.es)

## Abstract

This paper presents the integration of a conoscopic holography sensor (CH) in a machining centre (MC) by means of a centralized control on the machine's CNC (*CNC centralized control*). Besides the installation and extrinsic calibration of the sensor, the primary focus is the automation of the freeform digitizing process on the MC itself. To overcome the usual lack of compatibility between the respective interfaces of the CNC machine and the non-contact sensor, a system was developed to centralize the control intelligence on the machine's own CNC, enabling digitizing operations to be performed directly with the execution of an NC subroutine. In addition, three digitizing strategies are proposed: *Non-Adaptive*, *Adaptive* and *Predictive-Adaptive*. These require no planning tools or off-line programming prior to the digitizing process. The effectiveness of the extrinsic calibration method was validated by measuring a certified *ballbar*, and the integrated measuring system was checked by comparing the metrological results obtained by digitizing a freeform surface with those obtained by a CMM contact probe and with the CAD model used for machining the surface.

**Keywords:** CNC centralized control, freeform surface, digitizing, conoscopic holography

## **1 Introduction**

Inspection activities are of vital importance in today's industry to ensure that manufactured components meet design specifications. Inspection is usually carried out on CMM machines, owing to their high precision and measuring capacity. These machines require a considerable investment, however, and the need to move the component from the machine tool to the CMM leads to loss of precision and productivity.

To overcome these drawbacks, techniques have been developed to enable components to be measured directly on the same machine that manufactured them (On-Machine Measurement or OMM). In this way, production machines may be used for measurement purposes similarly to CMM contact probes, though metrological behaviour tends to be inferior.

Although many manufactured parts are designed using a combination of different primitive shapes (planes, cylinders, cones, spheres, etc.), more and more industrial sectors (automotive, aeronautics, energy, etc.) are demanding high-quality components that incorporate freeform surfaces. These characteristics, and even the size of the surface, mean that dimensional inspection requires data capture from a great number of points.

Measurement of freeform surfaces using CMMs is currently performed using algorithms of form deviation evaluation based on probe radius correction, which improves accuracy compared to methods based on direct use of nominal points [1].

Despite their precision, contact probes are not suitable for freeform surface digitizing in machine tools. Their main failings are their low data point capture rate, likely accessibility

problems, the need for probe tip radius correction, and the possibility of errors caused by tip wear, stylus bending, and even surface deformation at contact points [2], especially when digitizing soft materials.

Under such conditions, non-contact scanning techniques seem to be an advantageous alternative to contact methods since they allow for high acquisition rates, better accessibility conditions and, in many cases, similar levels of accuracy. Even so, the use of commercial non-contact measurement systems for OMM applications is still very limited. Many research works have studied the integration of non-contact sensors in production machines [3–5], but they have been primarily concerned with the installation of the sensor and calibration of the machine-sensor assembly, and have not tended to deal with the automation required to synchronize the running of both systems. A major difficulty to overcome is the considerable heterogeneity between the respective controllers of CNC machines and non-contact sensors, which renders the direct connection of such equipment for the synchronized operation of OMM tasks almost impossible.

Even if the interfaces were compatible, the majority of CNC controllers are not able to process the large amount of data captured by non-contact sensors. For this reason, most integration projects employ an auxiliary system which is responsible for coordinating operations between the CNC and the sensor, as well as processing and storing the data acquired during digitizing.

Typically, this auxiliary system consists of a computer in which a specific *master* application controls both the CNC and the sensor, which act as *slaves* (Fig. 1a). Although this control structure allows the coordinated running of both pieces of equipment to be automated, it is not a solution suited to the industrial environment, for two main reasons. Firstly, because the necessary programming tools, the application programming interface

(API), and the software development kit (SDK) must be available to develop the *master* application with the appropriate functionalities. Although such tools are widely available for non-contact sensors, the reverse is true for CNC machines, and some functionalities, such as the axes of movement of the machine, are practically reserved for open-structure CNCs [6]. Secondly, a computer must be used in conjunction with the CNC machine, and the machine operator requires specialized training to manage the developed application.

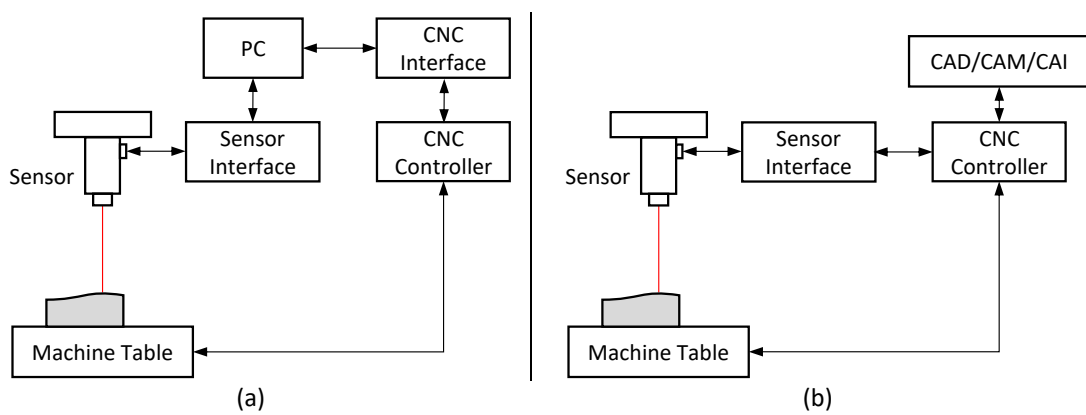


**Fig. 1** Control structures for automate operation: (a) PC centralized; (b) CNC centralized

If these systems are to have any practical application, then, the way in which the coordinated operations of the CNC controller and the non-contact sensor are automated needs to evolve, just as the integration of contact sensors in CNC machines has evolved [7]. In particular, a system is needed which will enable the non-contact sensor to be used as if it were merely another accessory of the machine. To achieve this, the control of the machine-sensor assembly must be centralized on the machine's CNC (*CNC centralized control*), enabling OMM tasks to be performed by running an NC routine directly from the CNC controller (Fig. 1b). Such an evolution would provide an *In-Cycle* measurement system similar to that currently used by contact measurement probes and would also facilitate the use of *Computer-Aided Inspection* (CAI) systems [8].

Many studies have focused on the optical factors that influence the metrological quality of non-contact sensor measurement results prior to their use for OMM. Worthy of note in this context are those which have studied the influence of the digitized point location within the sensor depth of field (DOF) on measurement results [5, 9–12]. All these studies note that digitizing is best performed within a narrow strip located at the centre of the sensor DOF.

This paper presents the integration of a non-contact, conoscopic holography (CH), digitizing sensor in a 3-axis machining centre (MC), applied to freeform surface digitizing by means of a *CNC centralized control*. Three phases of installation, extrinsic calibration and automation were developed, paying special attention to the compatibility of the system with the industrial environment. The effectiveness of the extrinsic calibration method was based on the measurements of a certified *ballbar*. During the automation phase, a system that centralizes the control intelligence on the machine's CNC was developed, allowing an operator to perform digitizing operations directly by running NC subroutines. The system can perform surface digitizing by using three different strategies (*Non-Adaptive*, *Adaptive* and *Predictive-Adaptive*) without either previous planning or using a CAD model. Finally, in order to verify the different strategies, a freeform surface was digitized under two of these, and the metrological results were compared with those obtained on a CMM by a contact probe and with the CAD model used to machine the surface.

## **2 System description**

### **2.1 Equipment**

The non-contact sensor used in this work was an Optimet™ ConoPoint-10 point-type

conoscopic holography sensor, to which it is possible to connect lenses with different focal length and DOF to adapt the sensor to different precision requirements. Two lenses of 25 and 50 mm focal length were used for this study. Table 1 shows the main characteristics of the CH sensor for both lenses [13]. It can be observed that a lens with a shallower DOF and shorter stand-off distance correlates to improved metrological performance. When using a sensor of this type integrated in a CNC machine for digitizing freeform surfaces, it is advisable to use a lens with a good metrological performance but with a stand-off distance long enough to avoid collisions.

**Table 1** Characteristics of the ConoPoint-10 CH sensor equipped with two different lenses

Characteristics	Lens 25 mm	Lens 50 mm
Depth of field, DOF (mm)	1.80	8
Stand-off (mm)	18	44
Linearity ( $\pm\%$ ) <sup>(1)</sup>	0.17	0.08
Repeatability ( $\mu\text{m}$ ) <sup>(2)</sup>	0.06	0.10
Laser spot size X <sup>(3)</sup> ( $\mu\text{m}$ )	20	37
Angular coverage ( $^\circ$ )	150	170
Dimensions ( $L \times W \times H$ ) (mm)	167 $\times$ 79 $\times$ 57	
Weight (g)	720	
Measuring frequency, $F$ (Hz)	up to 9000	
Power level, $P$ <sup>(4)</sup>	0 – 4095	

<sup>(1)</sup> The maximum relative measurement error over half the measurement ranges.

<sup>(2)</sup> Standard deviation of 10 consecutive measurements of a diffusive target, each lasting 0.6 seconds, at the sensor's stand-off distance.

<sup>(3)</sup> The full width at half maximum minimal value of the X beam axis in the measurement range, as measured by a beam profiler and after fitting the beam energy profile to a Gaussian distribution.

<sup>(4)</sup> Maximum power level is equivalent to 1 mW.

The CH sensor used in the experiments was integrated by the authors in a Lagun Lean L1000 3-axis machining centre with a FANUC M0i CNC controller and a Renishaw OMP400 contact probe for contact measurements. This is a vertical spindle MC with horizontal table movement (X,Y) and vertical head movement (Z).

## 2.2 Attachment of the CH sensor to the MC and extrinsic calibration of the equipment

The MC spindle was chosen to house the CH sensor to ensure the maximum possible capacity of relative and controlled movement between the sensor and the surface to be verified. A specific fixture was developed to easily connect or disconnect the sensor to the spindle by means of a standard cone (DIN 69871), as with any other tool (Fig. 2). The sensor position can be adjusted vertically by moving the Z axis of the MC, and the CH sensor also has the capacity to measure along the laser beam direction ( $Z_{CH}$ ) according to the DOF of the lens connected. In this way, points within the sensor's working range can be digitized without the need to adjust the MC Z axis. Furthermore, the Z axis can be moved to adapt the position of the sensor to the surface topography, so that all the points can be collected at a constant distance from the CH sensor (generally recommended at the stand-off distance).

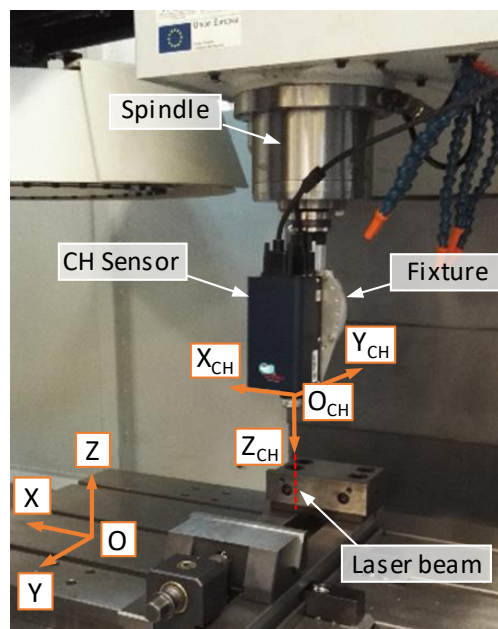


**Fig. 2** CH sensor connected to the MC spindle through a specific fixture and reference systems

The allocation of the CH sensor in the MC spindle enables its 3D movement within the working volume of the machine. As each point is digitized, the position of the MC axes is registered together with the distance-to-point ( $\gamma$ ) measured by the CH sensor, and the point coordinates must be expressed in terms that can be recognized by the MC reference system to enable the information to be used for metrological purposes. This is done by means of an extrinsic calibration procedure, inspired by the technique described in [14], once the CH sensor is attached to the spindle.

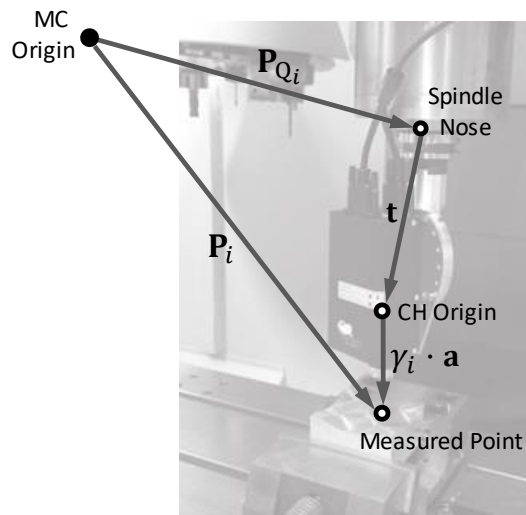


**Fig. 3** Vectors used for extrinsic calibration of the CH sensor

The CH sensor used is a point-type sensor, and therefore both the measurement direction ( $Z_{CH}$ ) and the internal CH sensor origin ( $O_{CH}$ ) must be related to the MC reference system during the extrinsic calibration process (Fig. 2). In this way, the offset between the sensor and MC origins will be determined and any misalignment between the laser beam ( $Z_{CH}$ ) and the MC vertical axis ( $Z$ ) corrected. In fact, the position of the spindle nose in relation to the MC origin is known, enabling the sensor origin to be related to the MC origin through this characteristic point. Two calibration vectors are used in this work to establish the geometric relationships (Fig. 3) [15]:



- $\mathbf{t}$ , which represents the offset of the CH origin with respect to the MC spindle nose.
- $\mathbf{a}$ , which is a unit vector aligned with the sensor measuring direction ( $Z_{CH}$ ). This vector, multiplied by the distance  $\gamma$  measured by the CH sensor, provides the vector that links the sensor origin with the measured point.

Therefore, for a digitized point  $i$ , if both the position of the MC spindle nose just at the instant of its capture ( $\mathbf{P}_{Q_i}$ ) and the distance measured by the CH sensor ( $\gamma_i$ ) are known, the point position ( $\mathbf{P}_i$ ) can be expressed to the MC reference system thus:

$$\mathbf{P}_i = \mathbf{P}_{Q_i} + \mathbf{t} + \gamma_i \cdot \mathbf{a} \quad (1)$$

The calibration vectors  $\mathbf{t}$  and  $\mathbf{a}$  are determined in this study by measuring a calibration sphere, a widely-available standard artefact with high geometric quality. The calibration procedure consists of using the CH sensor to measure a set of points distributed on the sphere, which is located on the MC table. At each point, both the distance  $\gamma_i$  measured by the sensor and the position of the spindle nose  $\mathbf{P}_{Q_i}$  are registered. Additional data required are the radius  $R_s$  of the sphere and the position of its centre  $\mathbf{C}_s$ , expressed according to the MC reference system. This data can be obtained using the contact probe in the MC. Alternatively, if using a calibrated sphere, the value of radius  $R_s$  can also be obtained from the calibration certificate.

Since the digitized points are captured on the surface of the sphere, assuming certain initial values of the calibration vectors  $\mathbf{t}$  and  $\mathbf{a}$ , a radius error of the sphere measured by the CH sensor can be calculated for each of these, using the following expression (Fig. 4):

$$\delta_i = R_{\text{meas}_i} - R_s = \left| \mathbf{P}_{Q_i} + \mathbf{t} + \gamma_i \cdot \mathbf{a} - \mathbf{C}_s \right| - R_s \quad (2)$$

By adding the quadratic errors of all digitized points on the sphere, an error function can be defined as follows:

$$f = \sum_{i=1}^n \delta_i^2 \quad (3)$$

where  $n$  is the number of digitized points.

By minimizing the value of this function, optimal values of the calibration vectors  $\mathbf{t}$  and  $\mathbf{a}$  can be obtained. Due to the non-linearity of this function, the Gauss-Newton iterative nonlinear least-square method was used in this case.

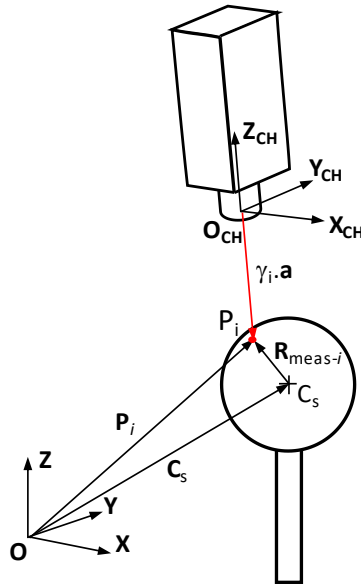


**Fig. 4** Relationship between the measured point  $P_i$  and the centre  $C_s$  of a test sphere

### 3 Validation of calibration results

In order to validate the developed calibration procedure, the CH sensor integrated in the MC was applied to the measurement of distances between the spheres of a certified *ballbar*, comparing results with the values on the certificate. The *ballbar* was composed of two ceramic spheres of good laser diffusion and nominal diameter of 20 mm (Fig. 5a),

attached to the ends of a carbon fibre bar at a certified distance of 249.53189 mm with uncertainty  $U = 1.05 \mu\text{m}$  ( $k = 2$ ) for a reference temperature of  $20 \text{ }^\circ\text{C}$ .

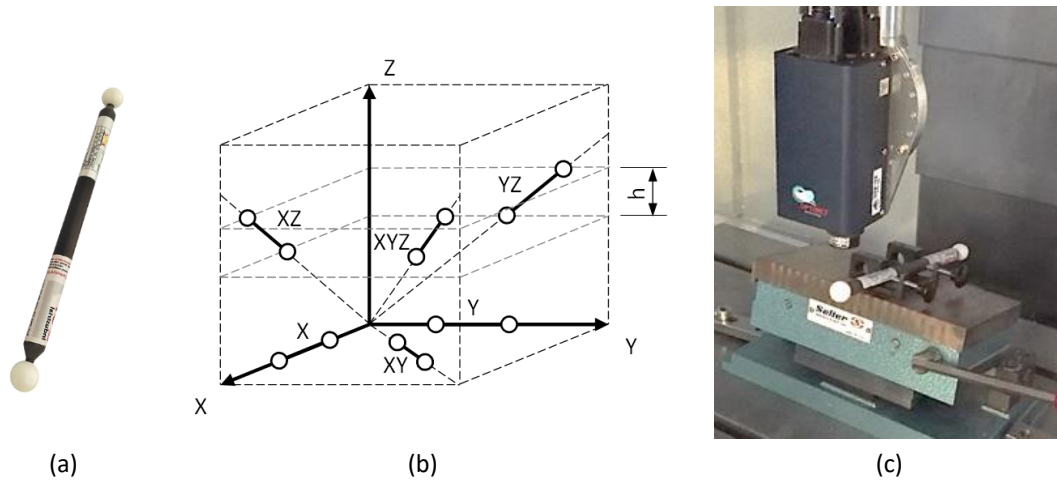


**Fig. 5** (a) *Ballbar*; (b) measured orientations; (c) measurement process in the MC

The artefact was arranged along six different directions within the MC working space in order to determine the influence of such orientations on the measurements (Fig. 5b). Those orientations with spheres at different Z were limited to a tilt angle of  $11.5^\circ$ , corresponding to a Z difference of 50 mm. This limitation was necessary to avoid occlusions of the laser, due to the interference of the cylindrical carbon fibre bar. The tilt angle was achieved by using a sine table (Fig. 5c).

The digitizing process with the CH sensor was performed using a lens with a focal length of 50 mm (Table 1), adjusting the sensor frequency to 3000 Hz and the power to 670 (0.164 mW). Five repetitions were performed under each orientation for digitizing the spheres, capturing 100 points per sphere (1000 repetitions on each point), distributed along a spiral over the top of the spheres, and covering a cone angle of  $120^\circ$ . During the digitizing of each ball, the Z position of the sensor remained constant. Its vertical position was adjusted initially to ensure that all the points lay within the lens DOF. Finally, each digitized sphere was reconstructed and the average value of 3D distances between their

centres and the standard deviations were calculated and compared to the values registered on the calibration certificate (Table 2).

**Table 2** Measurement results of the *ballbar* under different orientations and deviations from the certified value

	Orientation					
	X	Y	XY	XZ	YZ	XYZ
Distance (mm)	249.5290	249.5292	249.5293	249.5290	249.5289	249.5301
St. Dev. ( $\mu\text{m}$ )	0.61	0.48	0.45	0.60	0.59	0.52
Deviation ( $\mu\text{m}$ )	-2.9	-2.7	-2.6	-2.9	-3.0	-1.8

Table 2 shows that deviations of the distance measurements by the CH sensor from the certified value are always lower than  $3.0 \mu\text{m}$ , and the standard deviation over the 5 repetitions is lower than  $0.61 \mu\text{m}$  in all cases. This indicates very good precision in distance measurements and very low discrepancies with respect to the reference value. Thus, the calibration method proposed is valid to perform this type of measurement.

#### 4 Automation of the control process

The goal of this phase is to develop a system of automation of the inspection process using the CH sensor integrated in the machine. To facilitate installation of this inspection system in a generic industrial environment, automation needs to allow for the use of the sensor by executing an NC macro directly from the machine controller (*CNC centralized control*). This paper therefore proposes the use of an interface to connect the CH sensor and the MC controller, based on the following modules (Fig. 6):

- The *Switch*, which enables connection and communication between the sensor and the machine using the dynamic link libraries supplied by each manufacturer: *Smart32.dll* for the CH sensor and *FOCAS2* for the CNC. In addition, the *Switch* is able to acquire the data captured by the sensor and sends it to the *Data Processor*, together with information related to the extrinsic calibration of the sensor.

- The *Data Processor*, responsible for processing and converting all the digitizing data into metrological information suitable for OMM by applying extrinsic calibration. It also sends inspection results to the *Data Store*, along with the associated traceability data.
- The *Data Store*, responsible for storing the inspection results processed by the *Data Processor*.

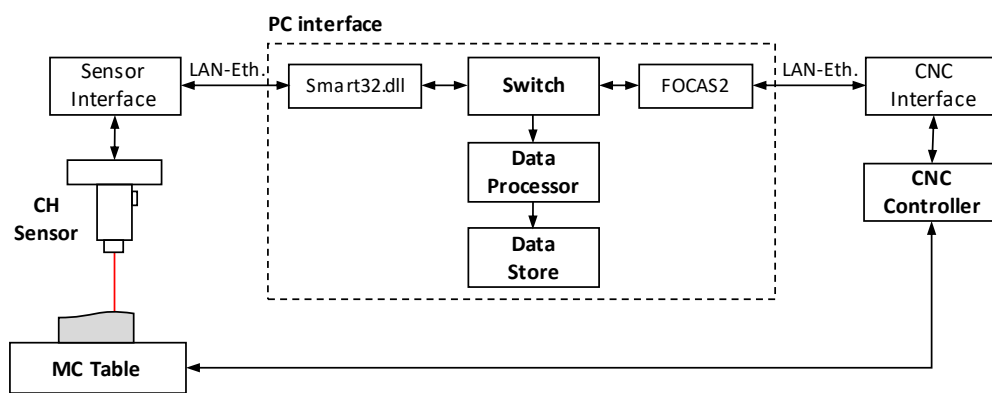


**Fig. 6** Connection interface between CH sensor and MC controller

The proposed interface in this work was implemented on a PC connected by LAN-Ethernet to both the CH sensor and the MC controller. Both the *Switch* module and the *Data Processor* are part of an application running autonomously on the PC, which starts up when the MC is switched on. The *Data Store* consists of a storage folder on the PC.

An NC macro is run as *master* on the CNC controller in order to centralize control on the CNC, with the CH sensor governed by the *Switch*, which acts as *slave* (Fig. 7). For this purpose, the macro assigns different values (Commands) to the variable #100 (*synchronization variable*), depending on the tasks that the CH sensor is to perform (Table 3). The *Switch* module constantly checks variable #100 and transmits the necessary instructions to the CH sensor (*Commands to Sensor*).

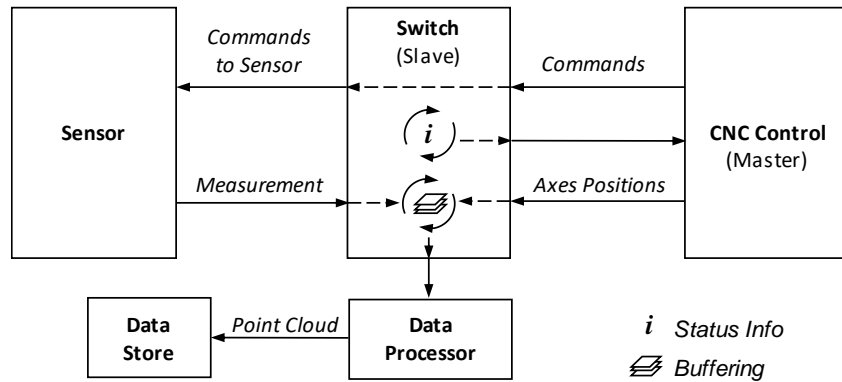


**Fig. 7** CNC centralized control process

**Table 3** Values of the synchronization variable and *Switch* actions

Command (#100)	Command to CH sensor
0	Wait for a new order
1	Configure the CH sensor
2	Capture measurements to adapt CH sensor position
3	Perform measurement with respect to the MC reference system
4	Finish digitizing

Figure 8 shows the flowchart for the main part of the NC macro that handles digitizing tasks, and Fig. 9 the flowchart for the *Switch* module. Both routines are executed simultaneously. Each time the value of the *synchronization variable* is changed by the NC macro to perform a digitizing task (values 1-4), the CNC remains waiting until the assigned task is completed by the *Switch*, which will then reset the *synchronization variable* to zero ( $\#100 = 0$ ) and return control to the CNC. When the NC macro assigns  $\#100 = 4$  to finish a digitizing task, the *Switch* module sends the inspection traceability data to the *Data Processor*: part number manufactured by the MC, date and time of the inspection, sensor configuration parameters, etc., all of which will be added to the measurement data.

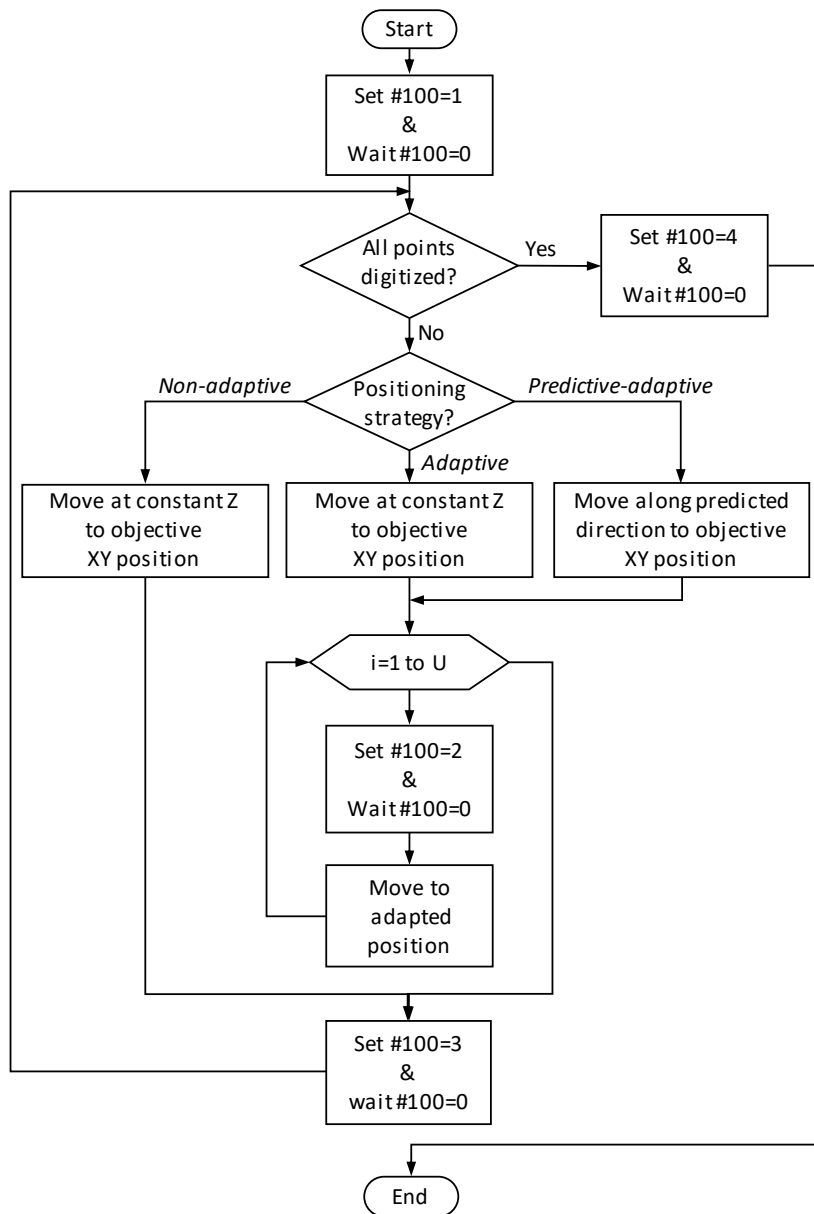


**Fig. 8** Flowchart of the NC digitizing macro

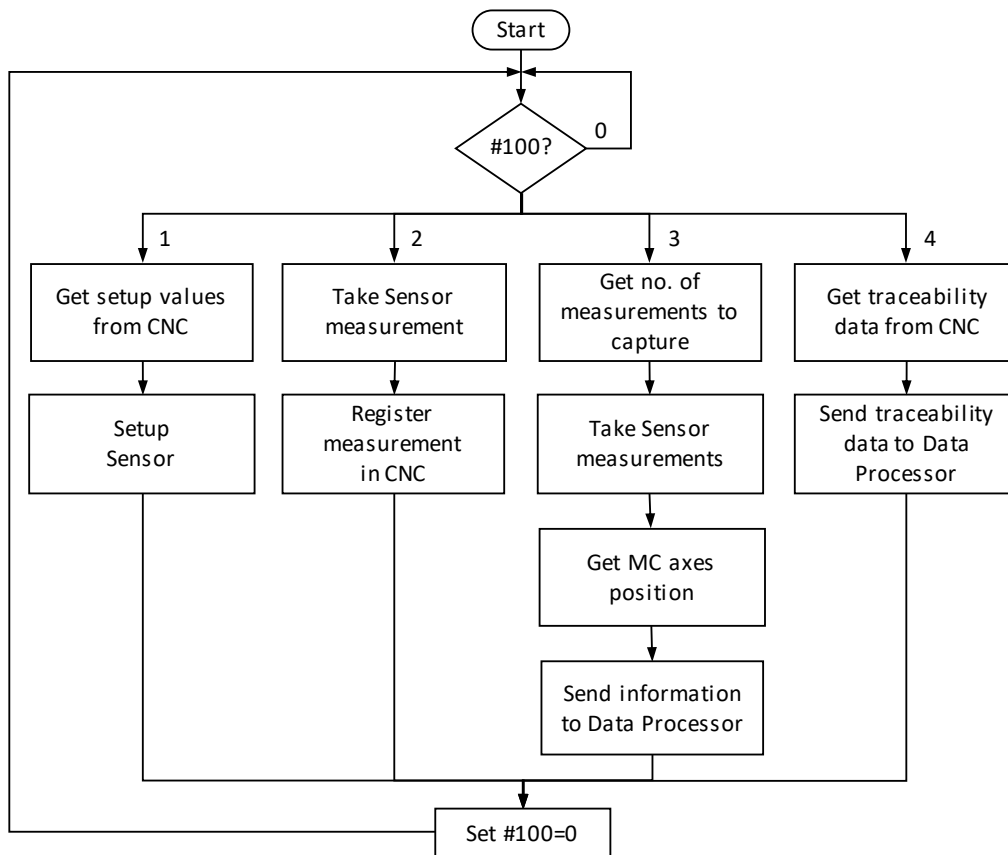


**Fig. 9** Flowchart of *Switch* module

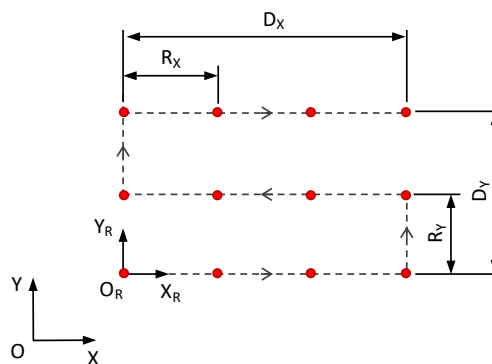


**Fig. 10** Distribution of points within the digitizing region

## 5 Digitizing procedure

This section will address the practicalities for the user performing the digitizing process with the NC macro. Initially, the general parameters must be specified, such as the coordinates of the starting point for digitizing, the feed rate, and a safety height to avoid



collisions. From this information, the macro performs a point-to-point digitizing of a rectangular region in which the points are distributed along parallel lines to X direction (Fig. 10). This is carried out through a specifically developed cycle (P1120) called from the macro by function G65 ("custom macro simple call"), as follows:

$$G65 P1120 D E F H M Q R U V W X Y Z \quad (4)$$

The parameters are detailed in Table 4.

**Table 4** Parameters of the digitizing cycle P1120

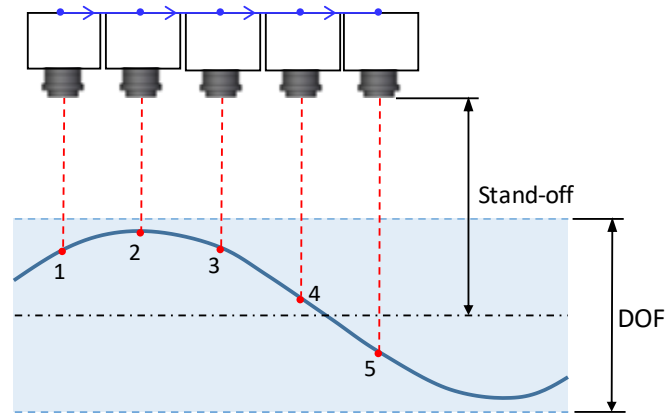
		Parameter				
Type		Id.	Description	Value	Defect value	Unit
Mandatory	Digitizing	D	D <sub>X</sub>	> 0	-	mm
		E	D <sub>Y</sub>	> 0	-	mm
		F	R <sub>X</sub>	> 0	-	mm
		H	R <sub>Y</sub>	> 0	-	mm
	MC	M	Feed Rate	[1, 30000]	-	mm/min
		Q	Safety Z (MC system)	[5, -495]	-	mm
Mode	R		Non-Adaptive	0	-	-
			Adaptive	1		
			Predictive-Adaptive	2		
Optional	CH	U	No. adaptations	≥ 1	1	-
		V	DOF Position	[0, 100]	50	%
		W	Frequency	[0, 9000]	3000	Hz
		X	Power	[0, 4095]	2000	-
		Y	Auto Exposure	0, 1	0	-
		Z	Captures per point	> 1	1000	-

Cycle P1120 enables digitizing by means of three sensor positioning strategies at each point: *Non-Adaptive* (R = 0), *Adaptive* (R = 1), and *Predictive-Adaptive* (R = 2).

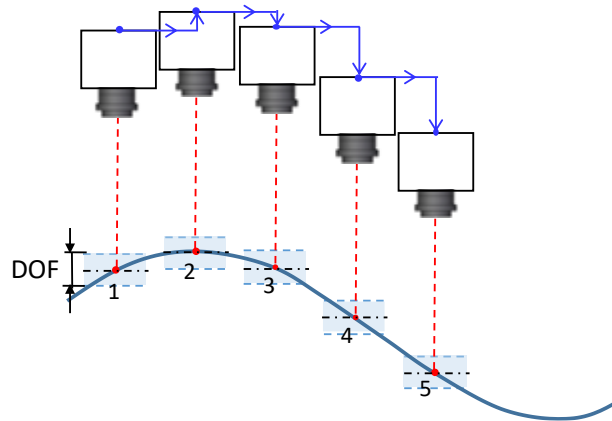
- *Non-Adaptive* (Fig. 11a): As the sensor moves, its position Z remains invariable along all the points to be digitized. A lens with sufficient DOF to be able to capture all the

surface points is needed. Under this strategy, it is not possible to ensure that all points are acquired at the stand-off distance of the sensor.

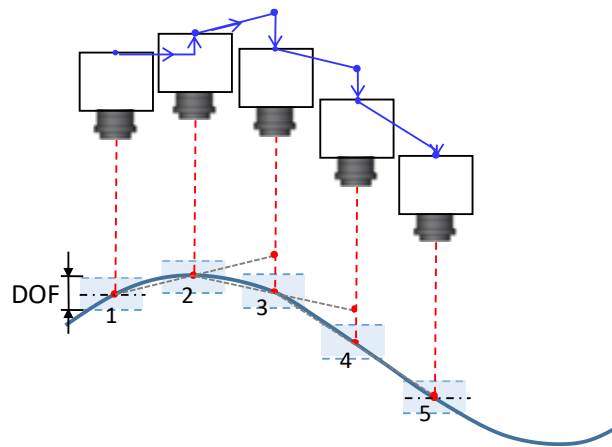
- *Adaptive* (Fig. 11b): The Z position of the sensor at each point of the surface is adapted to maintain a uniform distance between the sensor and the point. The distance value must be specified initially to ensure that all points will be acquired at a specific position within the DOF (Fig. 12). During the digitizing procedure, the sensor moves with no Z variation until it reaches the position of the next point, where it is displaced along the laser beam direction (vector  $\mathbf{a}$ ) until the distance between the sensor and the digitized point meets the value defined by parameter V of the cycle. This ensures that all the points are captured at the same position within the DOF. This adjustment process can be repeated at each point as many times as set by parameter U of the cycle.
- *Predictive-Adaptive* (Fig. 11c): As with the previous strategy, the objective is to digitize all the points at the same position within the DOF, initially defined by parameter V, but using a slightly different sensor positioning technique. To position the sensor at a certain point (i.e. point 3), the previous two digitized points (i.e., 1 and 2) are taken into account. Following a direction parallel to the line joining both points, the sensor is then moved to the XY position of the new point. From this position, it is displaced along the laser beam direction (vector  $\mathbf{a}$ ) until the distance between the sensor and the digitized point meets the value of parameter V. This procedure is applicable to all points except the first and the second, which require positioning in *Adaptive* mode.



(a) Non-adaptive ( $R=0$ )



(b) Adaptive ( $R=1$ )



(c) Predictive-adaptive ( $R=2$ )

**Fig. 11** Movement strategies of the CH sensor for digitizing

The *Predictive-Adaptive* strategy is less time-consuming than the *Adaptive* procedure in areas with no major curvature changes. Better productivity can therefore be achieved when digitizing surfaces which require an elevated number of capture points.

Notwithstanding, the final sensor position at each point is identical in both strategies, and therefore no metrological differences will be observed between them, irrespective of the lens used. By contrast, the *Non-Adaptive* strategy requires the lens DOF to be deep enough for all the surface points to lie within it. There may be limitations of precision with this strategy, particularly when a deeper lens DOF is required.

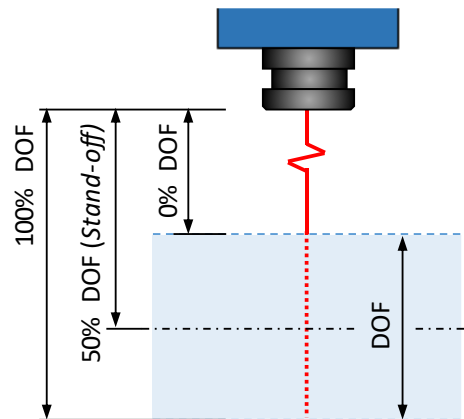


**Fig. 12** Definition of DOF positions

## 6 Case study: digitizing of a freeform surface

To evaluate the metrological quality of the results obtained with the CH sensor integrated in the MC and its applicability to OMM, digitizing tests of a freeform surface were carried out using two lenses with different DOF (50 and 25 mm) and under two different strategies: *Non-Adaptive* and *Predictive-Adaptive* at 50% DOF. The *Adaptive* strategy was not tested since the capture conditions are identical to those under the *Predictive-Adaptive* strategy and provide the same metrological results. The surface was also digitized on a CMM by means of a contact probe with a 2 mm tip.

The freeform surface was milled in the MC from an aluminium 6061 stock of 90x90x45 mm<sup>3</sup> with an average roughness Ra of 0.8 µm. The whole surface lay within a range of 7 mm on Z (Fig. 13a).

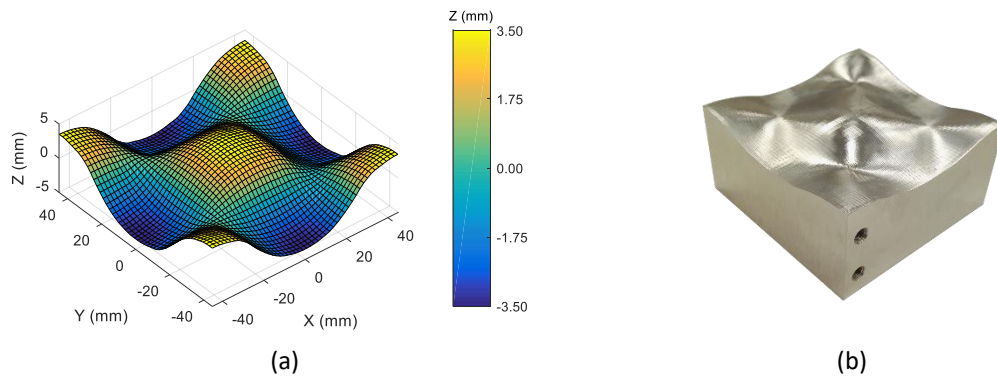


**Fig. 13** Freeform surface: (a) model; (b) machined

In all cases, the digitizing performed covered an area of  $80 \times 80 \text{ mm}^2$ , by capturing 6561 points with a resolution of 1 mm along both X and Y directions. The input parameters for the cycle P1120 of the NC macro are shown in Table 5. The W and X parameters corresponding to the frequency and power of the CH sensor were chosen to provide a quality acquisition signal within the operating limits of the sensor (Table 1).

**Table 5** Values of the digitizing cycle parameters used in the tests

	Parameter												
	D	E	F	H	M	Q	R	U	V	W	X	Y	Z
Value	80	80	1	1	1000	-220	0 / 2	1	50	2000	4000	1	400

To analyse the results, the point clouds obtained in each test were compared with the surface CAD model. First, alignment of each point cloud with the CAD model was performed using an ICP algorithm (Iterative Closest Point) available in MATLAB. Next, the distance from each digitized point to the theoretical surface along its normal direction was calculated. This distance represents the error detected between the digitized surface and the model. The error evaluation method follows ISO 1101 recommendations for profile tolerance verification of a surface not related to a datum [16]. Figure 14 shows the distribution of errors detected in each case by means of the RMS (Root Mean Square),

standard deviation ( $\sigma$ ) and range.

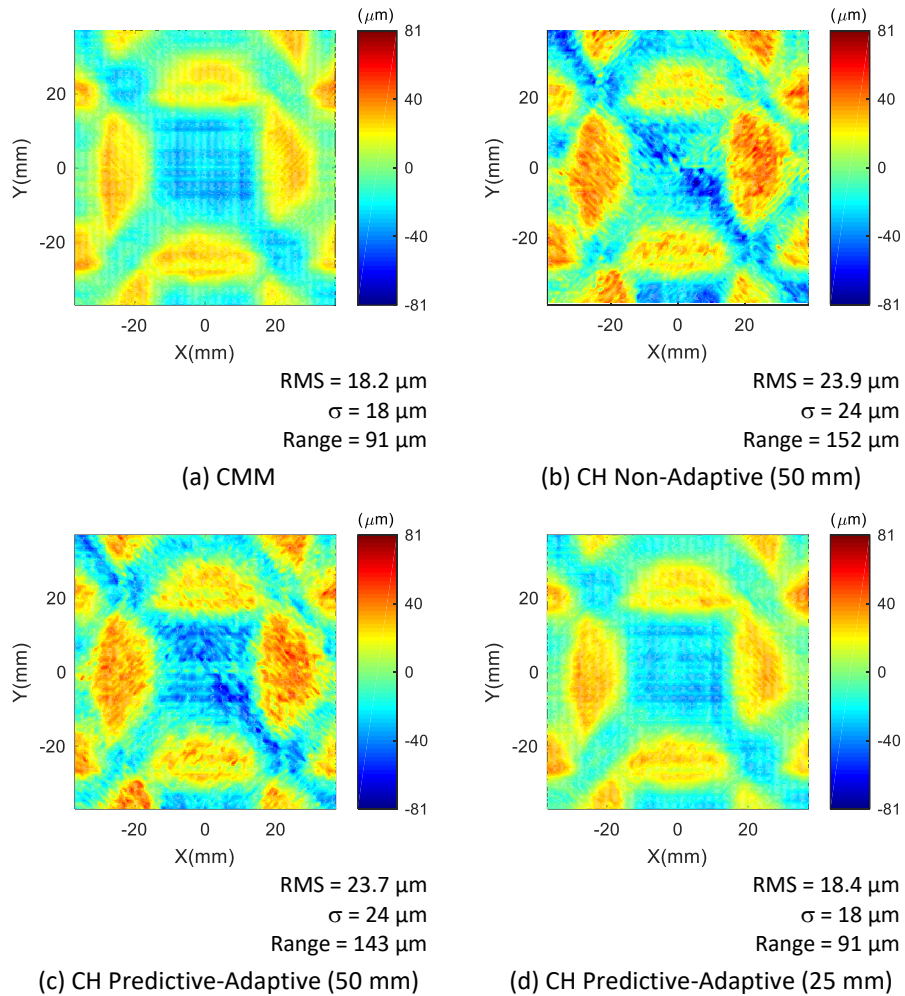


**Fig. 14** Errors detected in each test with respect to the surface model

As can be observed, the distributions of detected errors with respect to the theoretical surface show a similar pattern of errors in all the tests; areas with excess and lack of material are therefore coincidental. Notable similarity can be observed, however, between the error maps corresponding to the two digitizing tests performed with the 50 mm lens (Fig. 14b and 14c), and between the CMM and the 25 mm lens (Fig. 14a and 14d). To analyse these similarities in more detail, Fig. 15 shows the difference between the errors when comparing the two tests carried out with the 50 mm lens and when comparing the

CMM and the 25 mm lens. In both cases, very small RMS and  $\sigma$  values indicate that the errors were similar.

Comparing the maps by zones, the most notable differences in Fig. 15a correspond to those areas of the surface where the digitized points with the *Non-Adaptive* strategy are further away from the stand-off of the sensor lens. Fig. 15b indicates that positive differences are mainly found in convex areas of the surface, whereas negative differences correspond to the concave areas. This may be due to variations in the optical behaviour of material as a function of curvature (i.e. brightness or laser beam incident angle).

In view of these results, it can be stated that:

- No significant differences are observed between the *Non-Adaptive* and the *Predictive-Adaptive* methods when using the CH sensor with the 50 mm lens.
- The best scanning results with the CH sensor were obtained with the *Predictive-Adaptive* strategy using a 25 mm lens, being similar to those obtained in the CMM with the contact probe.

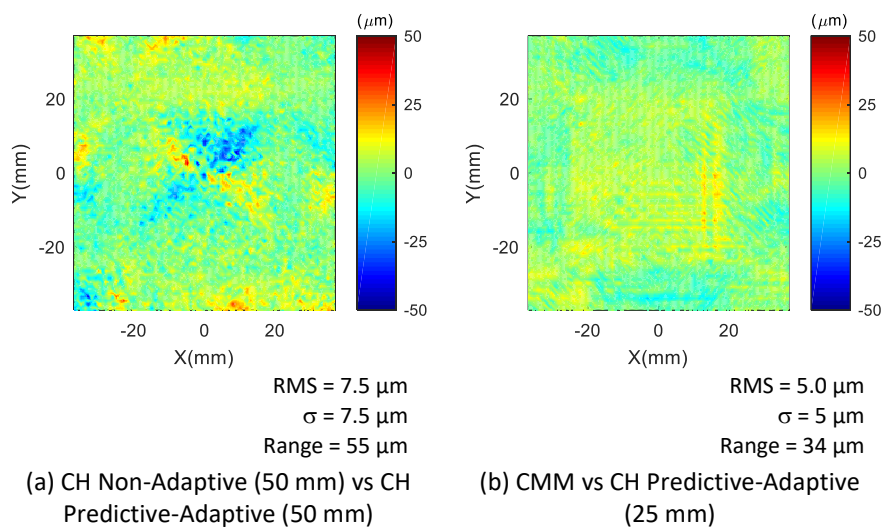


**Fig. 15** Difference of errors between the most similar strategies

## 7 Conclusions

This study integrated a point-type CH sensor in a 3-axis MC, using CNC centralized operation to perform digitizing of freeform surfaces machined on the same machine tool. Besides installation and extrinsic calibration of the sensor, essential to any integration, special attention was paid to the automation of coordinated machine-sensor operation, in order to meet the needs of the industrial environment. For this purpose, a system was developed to perform the digitizing process by simply running an NC macro directly from the machine tool controller (*CNC centralized control*), with no special expertise required by the operator. An interface based on three modules (*Switch, Data Processor, Data Store*) was developed and implemented on a PC, to enable the connection between the CH sensor and the MC controller. The NC macro used a cycle (P1120) that allows digitizing to be performed under three different strategies: *Non-Adaptive, Adaptive* and *Predictive-Adaptive*.

The results obtained with the integrated CH sensor were compared to those obtained by a CMM machine contact probe, both for validation purposes and to determine the utility of the integrated sensor in digitizing freeform surfaces. The metrological quality of the information captured by the integrated system demonstrates values very similar to those obtained by the CMM, especially under the *Predictive-Adaptive* strategy with a lens of 25 mm focal length. The use of lenses with a shorter focal length could produce even better metrological results.

Finally, the results indicate that the CH sensor integrated in a MC is able to digitize freeform surfaces using a cycle implemented directly from the CNC control.



## **Acknowledgements**

This work was supported by the Regional Ministry of Economy and Employment of the Principality of Asturias (Spain) (GRUPIN14-063) and the Government of the Principality of Asturias through the Programme “Severo Ochoa” 2014 of PhD grants for research and teaching (BP14-049).

## **References**

- [1] Magdziak M. An algorithm of form deviation calculation in coordinate measurements of free-form surfaces of products. *Journal of Mechanical Engineering* 2016; 62(1): 51-59.
- [2] Mutilba U, Gómez-Acedo E, Kortaberria G, Olarra A, Yagüe-Fabra JA. Traceability of On-Machine Tool Measurement: A Review. *Sensors* 2017; 17(7): 1605.
- [3] Shiou FJ, Chen MJ. Intermittent process hybrid measurement system on the machining centre. *International Journal of Production Research* 2003; 41(18): 4403–4427.
- [4] Qiu H, Nisitani H, Kubo A, Yue Y. Autonomous form measurement on machining centers for free-form surfaces. *International Journal of Machine Tools and Manufacture* 2004; 44(9): 961–969.
- [5] Li B, Li F, Liu HQ, Cai H, Mao XY, Peng FY. A measurement strategy and an error-compensation model for the on-machine laser measurement of largescale free-form surfaces. *Meas. Sci. Technol.* 2014; 25(1): 1–11.

- [6] Ko TJ, Park JW, Kim HS, Kim SH. On-machine measurement using a noncontact sensor based on a CAD model. *International Journal of Advanced Manufacturing Technology* 2007; 32(7–8): 739–746.
- [7] Kim KD, Chung SCh. Synthesis of the measurement system on the machine tool. *International Journal of Production Research* 2001; 39(11): 2475–2497.
- [8] Zhou EP, Harrison DK, Link D. Effecting in-cycle measurement with preteritic CNC machine tools. *Computers in Industry* 1996; 28(2): 95–102.
- [9] Isheil A, Gonnet J-P, Joannic D, Fontaine J-F. Systematic error correction of a 3D laser scanning measurement device. *Optics and Lasers in Engineering* 2011; 49(1): 16–24.
- [10] Van Gestel N, Cuypers S, Bleys P, Kruth J-P. A performance evaluation test for laser line scanners on CMMs. *Optics and Lasers in Engineering* 2009; 47(3–4): 336–342.
- [11] Feng H-Y, Liu Y, Xi F. Analysis of digitizing errors of a laser scanning system. *Precision Engineering* 2001; 25(3): 185–191.
- [12] Fernández P, Blanco D, Rico C, Valiño G, Mateos S. Influence of surface position along the working range of conoscopic holography sensors on dimensional verification of AISI 316 wire EDM machined surfaces. *Sensors* 2014; 14(3): 4495–4512.
- [13] ConoPoint Series User Manual, Optimet P/N 3J06009 (Accessed Sep. 12 2015) <http://www.optimet.com>.
- [14] Zapico P, Fernández P, Rico JC, Valiño G, Patiño H. Extrinsic calibration of a conoscopic holography system integrated in a CMM. *Precision Engineering* 2018; 52: 484-493.

- [15] Smith KB, Zheng YF. Point laser triangulation probe calibration for coordinate metrology. *Journal of Manufacturing Science and Engineering* 2000; 122(3): 582–586.
- [16] ISO 1101, 2017. Geometrical product specifications (GPS)—Geometrical tolerancing—Tolerances of form, orientation, location and run-out.